Inorg. Chem. **2007**, *46*, 9234–9244

Applications of Bis(1-R-imidazol-2-yl)disulfides and Diselenides as Ligands for Main-Group and Transition Metals: κ^2-(N,N) Coordination, S–S Bond Cleavage, and S–S/E–E (E = S, Se) Bond Metathesis Reactions

Joshua S. Figueroa, Kevin Yurkerwich, Jonathan Melnick, Daniela Buccella, and Gerard Parkin*

Department of Chemistry, Columbia University, New York, New York 10027

Received June 22, 2007

Bis(1-R-imidazol-2-yl)disulfides, $(mim^R)_2$ (R = Ph, Bu^t), and diselenides, $(seim^{Mes})_2$, serve as bidentate N,N-donor ligands for main-group and transition metals. For example, $[\kappa^2\text{-}(mim^{Bu^t})_2]MCl_2$ (M = Fe, Co, Ni, Zn), $[\kappa^2\text{-}(mim^{Ph})_2]MCl_2$ (M = Co, Zn), $[\kappa^2\text{-}(mim^{Bu^t})_2]CuX$ (X = Cl, I), and $[\kappa^2\text{-}(seim^{Mes})_2]MCl_2$ (M = Fe, Co, Ni) are obtained by treatment of $(mim^{Bu^t})_2$ or $(seim^{Mes})_2$ with the respective metal halide and have been structurally characterized by X-ray diffraction. On the other hand, the zerovalent nickel complex $Ni(PMe_3)_4$ effects cleavage of the disulfide bond of $(mim^{Bu^t})_2$ to give square-planar *trans*-$Ni(PMe_3)_2(mim^{Bu^t})_2$ in which the (mim^{Bu^t}) ligands coordinate via nitrogen rather than sulfur, a most uncommon coordination mode for this class of ligands. Although $[\kappa^2\text{-}(mim^R)_2]MCl_2$ (M = Fe, Co, Ni, Zn) are not subject to homolytic cleavage of the S–S bond because the tetravalent state is not readily accessible, the observation that $[\kappa^2\text{-}(mim^{Ph})_2]CoCl_2$ and $[\kappa^2\text{-}(mim^{Bu^t})_2]CoCl_2$ form an equilibrium mixture with the asymmetric disulfide $[\kappa^2\text{-}(mim^{Ph})(mim^{Bu^t})]CoCl_2$ indicates that S–S bond cleavage via another mechanism is possible. Likewise, metathesis between disulfide and diselenide ligands is observed in the formation of $[\kappa^2\text{-}(mim^{Bu^t})(seim^{Mes})]CoCl_2$ upon treatment of $[\kappa^2\text{-}(mim^{Bu^t})_2]CoCl_2$ with $[\kappa^2\text{-}(seim^{Mes})_2]CoCl_2$.

Introduction

Current interest in metal thiolate chemistry derives to a large extent from the roles that such motifs, most commonly involving cysteine residues, play in biological systems.[1] In this regard, it is important to emphasize that the function of a biological thiolate is not merely to serve as a ligand, because the sulfur itself is also a site of critical reactivity. For example, cysteine ligands are subject to attack by electrophiles (as exemplified by the Ada DNA repair protein) and are also redox-active.[2] With respect to the redox activity of cysteine ligands, a common transformation involves the reversible formation of a disulfide bond, a conversion that plays a role in protein folding and cell signaling;[2,3] furthermore, the disulfide linkage may also serve as a ligand for metals in proteins.[4,5] While cysteine is also a common component of intracellular thiols (e.g., glutathione, tropanothione, and mycothiol), there is also a class of aromatic thiols that are derived from histidine, of which ergothioneine

* To whom correspondence should be addressed. E-mail: parkin@columbia.edu.

(1) (a) Solomon, E. I.; Gorelsky, S. I.; Dey, A. *J. Comput. Chem.* **2006**, *27*, 1415−1428. (b) Dance, I. G. *Polyhedron* **1986**, *5*, 1037−1104. (c) Block, E.; Zubieta, J. *Adv. Sulfur Chem.* **1994**, *1*, 133−193. (d) González-Duarte, P. In *Comprehensive Coordination Chemistry II*; McCleverty, J. A., Meyer, T. J., Eds.; Elsevier: Oxford, U.K., 2004; Chapter 8.9. (e) Henkel, G.; Krebs, B. *Chem. Rev.* **2004**, *104*, 801−824. (f) Rao, P. V.; Holm, R. H. *Chem. Rev.* **2004**, *104*, 527−559. (g) Sellmann, D. *New J. Chem.* **1997**, *21*, 681−689. (h) Belle, C.; Rammal, W.; Pierre, J.-L. *J. Inorg. Biochem.* **2005**, *99*, 1929−1936. (i) Stillman, M. J. *Coord. Chem. Rev.* **1995**, *144*, 461−511.

(2) (a) Giles, N. M.; Giles, G. I.; Jacob, C. *Biochem. Biophys. Res. Commun.* **2003**, *300*, 1−4. (b) Jacob, C. *Nat. Prod. Rep.* **2006**, *23*, 851−863. (c) Hand, C. E.; Honek, J. F. *J. Nat. Prod.* **2005**, *68*, 293−308. (d) Biswas, S.; Chida, A. S.; Rahman, I. *Biochem. Pharmacol.* **2006**, *71*, 551−564. (e) Giles, N. M.; Watts, A. B.; Giles, G. I.; Fry, F. H.; Littlechild, J. A.; Jacob, C. *Chem. Biol.* **2003**, *10*, 677−693. (f) Jacob, C.; Knight, I.; Winyard, P. G. *Biol. Chem.* **2006**, *387*, 1385−1397. (g) Jacob, C.; Giles, G. I.; Giles, N. M.; Sies, H. *Angew. Chem., Int. Ed.* **2003**, *42*, 4742−4758. (h) Raina, S.; Missiakas, D. *Annu. Rev. Microbiol.* **1997**, *51*, 179−202. (i) Maret, W. *Biochemistry* **2004**, *43*, 3301−3309.

(3) In addition to S−S bond formation, thiolates participate in a variety of other redox transformations. See, for example, ref 2 and Grapperhaus, C. A.; Darensbourg, M. Y. *Acc. Chem. Res.* **1998**, *31*, 451−459.

(4) Banci, L.; Bertini, I.; Calderone, V.; Ciofi-Baffoni, S.; Mangani, S.; Martinelli, M.; Palumaa, P.; Wang, S. *Proc. Nat. Acad. Sci.* **2006**, *103*, 8595−8600.

(5) The coordination chemistry of organodisulfides has been widely studied. See: Carrillo, D. *Coord. Chem. Rev.* **1992**, *119*, 137−169.

10.1021/ic701228y CCC: $37.00
Published on Web 09/28/2007

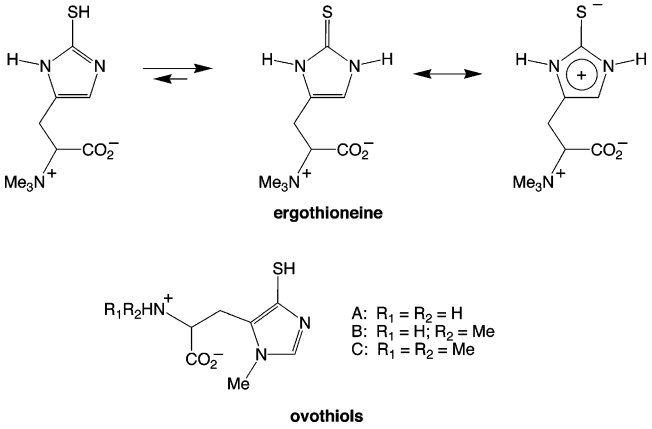

Figure 1. Structures of ergothioneine and ovothiols.

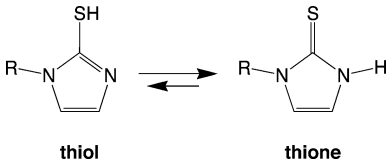

Figure 2. Thiol/thione tautomerism for 1-R-2-mercaptoimidazoles. The resonance-stabilized thione form is more stable.

and ovothiols are representative (Figure 1).[2b,c,6] The disulfides of ergothioneine and ovothiols[7] are known, but their chemistry has not been thoroughly investigated and their ligating properties are unknown. Therefore, we describe herein the applications of compounds that are structurally related to ergothioneine disulfide, namely, bis(1-R-imidazol-2-yl)-disulfides, to the chemistry of main-group and transition metals.

Results and Discussion

1. Bis(1-R-imidazol-2-yl)disulfides as Models for Ergothioneine Disulfide. Ergothioneine is a derivative of 2-mercaptoimidazole and exists primarily as the resonance-stabilized thione tautomer (Figure 1).[6] As such, essential features of its chemistry may be modeled by investigating simpler 1-R-2-mercaptoimidazole/1-R-imidazole-2-thione systems, which are also subject to such tautomerization (Figure 2) and primarily exist in the resonance-stabilized thione form. With respect to ergothioneine disulfide, it is pertinent to note that although the analogues bis(1-R-imidazol-2-yl)disulfides (R = H, Me, Ph, Bu^t), herein abbreviated as $(mim^R)_2$, are long known,[8] their application as ligands is virtually nonexistent. In fact, we are aware of only a single metal compound that contains the $(mim^R)_2$ ligand, namely, the zinc derivative $[\kappa^2\text{-}(mim^{Me})_2]ZnCl_2$.[9]

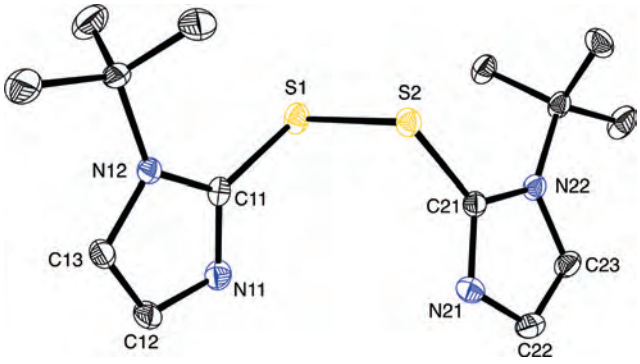

Figure 3. Molecular structure of $(mim^{Bu^t})_2$.

Scheme 1

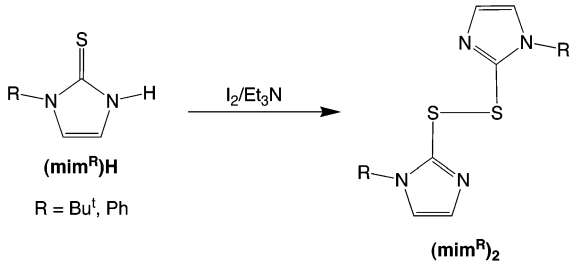

However, this complex was *not* obtained by using the disulfide $(mim^{Me})_2$ as a reagent; rather, $[\kappa^2\text{-}(mim^{Me})_2]ZnCl_2$ was only isolated as a side product in 4% yield resulting from adventitious oxidation of methimazole $(mim^{Me})H$ during the reaction with $ZnCl_2$ over a period of several months at 0 °C.[9] It is, therefore, evident that a deliberate investigation of the reactivity of the disulfides $(mim^R)_2$ towards metal compounds is warranted.

While a variety of $(mim^R)_2$ derivatives are available,[8] the synthetic method used to prepare the *tert*-butyl derivative $(mim^{Bu^t})_2$ is not described in the original report of this compound.[8b] Access to the yellow-orange disulfide $(mim^{Bu^t})_2$ is, nevertheless, readily achieved by oxidation of 1-*tert*-butylimidazole-2-thione, $(mim^{Bu^t})H$,[10] with I_2 (0.5 equiv) in the presence Et_3N (Scheme 1).[11] The phenyl derivative $(mim^{Ph})_2$ is likewise obtained from the corresponding reaction of $(mim^{Ph})H$[12] with I_2 and Et_3N. The molecular structures of $(mim^{Bu^t})_2$ and $(mim^{Ph})_2$ have been determined by X-ray diffraction, as illustrated in Figures 3 and 4. Selected metrical data are listed in Table 1, but noteworthy features are that (i) the S−S and S−C bonds are typical of single bonds,[13] (ii) the two C_{ipso}−N bond lengths in each (mim^R) fragment are different and are in accord with a resonance structure in

(6) (a) Hand, C. E.; Taylor, N. J.; Honek, J. F. *Bioorg. Med. Chem. Lett.* **2005**, *15*, 1357−1360. (b) Chaudiere, J.; Ferrari-Iliou, R. *Food Chem. Toxicol.* **1999**, *37*, 949−962.

(7) (a) Heath, H.; Toennies, G. *Biochem. J.* **1958**, *68*, 204−210. (b) Selman-Reimer, S.; Duhe, R. J.; Stockman, B. J.; Selman, B. R. *J. Biol. Chem.* **1991**, *266*, 182−188. (c) Turner, E.; Klevit, R.; Hopkins, P. B.; Shapiro, B. M. *J. Biol. Chem.* **1986**, *261*, 13056−13063. (d) Shapiro, B. M.; Hopkins, P. B. *Adv. Enzymol. Relat. Areas Mol. Biol.* **1991**, *64*, 291−316.

(8) See, for example: (a) Arnold, H.; Vogelsang, D. German Patent DE 960279, 1957. (b) Corey, E. J.; Brunelle, D. J. *Tetrahedron Lett.* **1976**, *17*, 3409−3412. (c) Freeman, F.; Keindl, M. C.; Po, H. N.; Brinkman, E.; Masse, J. A. *Synthesis* **1989**, *9*, 714−715.

(9) Matsunaga, Y.; Fujisawa, K.; Amir, N.; Miyashita, Y.; Okamoto, K. *Appl. Organomet. Chem.* **2005**, *19*, 208.

(10) Cassidy, C. S.; Reinhardt, L. A.; Cleland, W. W.; Frey, P. A. *J. Chem. Soc., Perkin Trans. 2* **1999**, 635−641.

(11) Oxidation of thiols to disulfides using I_2 is well precedented. See, for example: (a) Small, L. D.; Bailey, J. H.; Cavallito, C. J. *J. Am. Chem. Soc.* **1947**, *69*, 1710−1713. (b) Zeynizadeh, B. *J. Chem. Res. (S)* **2002**, 564−566.

(12) Matsuda, K.; Yanagisawa, I.; Isomura, Y.; Mase, T.; Shibanuma, T. *Synth. Commun.* **1997**, *27*, 3565−3571.

(13) The average S−S and S−C(sp^2) single bond lengths for compounds listed in the Cambridge Structural Database (version 5.28) are 2.05 and 1.74 Å, respectively. Allen, F. H.; Kennard, O. 3D Search and Research Using the Cambridge Structural Database. *Chem. Des. Autom. News* **1993**, *8* (1), 1 and 31−37.

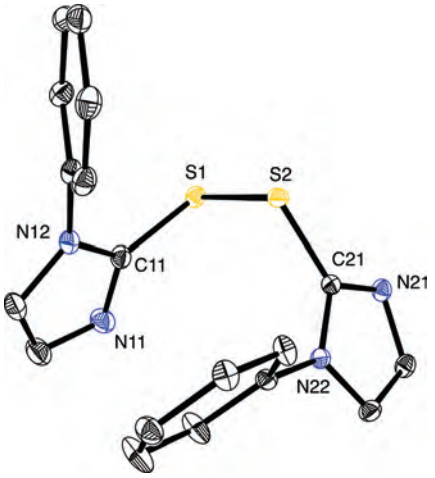

Figure 4. Molecular structure of $(mim^{Ph})_2$.

Table 1. Selected Metrical Data for $(mim^{But})_2$ and $(mim^{Ph})_2$

	$(mim^{But})_2$	$(mim^{Ph})_2$
S1−S2/Å	2.0807(9)	2.0699(4)
S1−C11/Å	1.747(2)	1.749(1)
S2−C21/Å	1.748(2)	1.743(1)
C11−N11/Å	1.319(3)	1.321(1)
C11−N12/Å	1.381(3)	1.373(2)
N11−C12/Å	1.362(3)	1.373(2)
C12−C13/Å	1.355(3)	1.365(2)
C13−N12/Å	1.364(3)	1.380(1)
C21−N21/Å	1.318(3)	1.330(1)
C21−N22/Å	1.379(3)	1.376(1)
N22−C23/Å	1.365(3)	1.375(1)
C22−C23/Å	1.356(4)	1.379(1)
C23−N22/Å	1.365(3)	1.375(1)
C11−S1−S2−C21/deg	93.1	83.7

Scheme 2

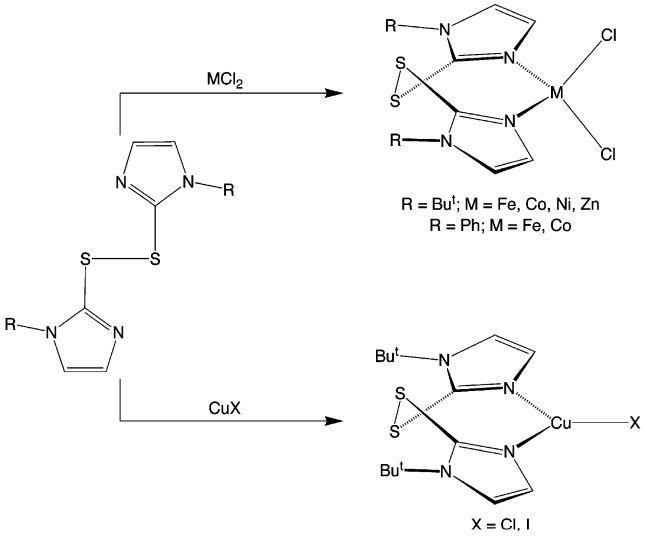

which the C═N double bond is more localized between the *ipso* carbon atom and the unsubstituted nitrogen atom (Scheme 1), and (iii) the C−S−S−C torsion angles are approximately 90°, in accord with an orientation that minimizes repulsions between the lone pairs on the two sulfur atoms.[5]

The disulfides $(mim^R)_2$ are effective bidentate ligands for a variety of metals, binding through two of the imidazolyl nitrogen atoms. For example, $(mim^R)_2$ coordinates to a series

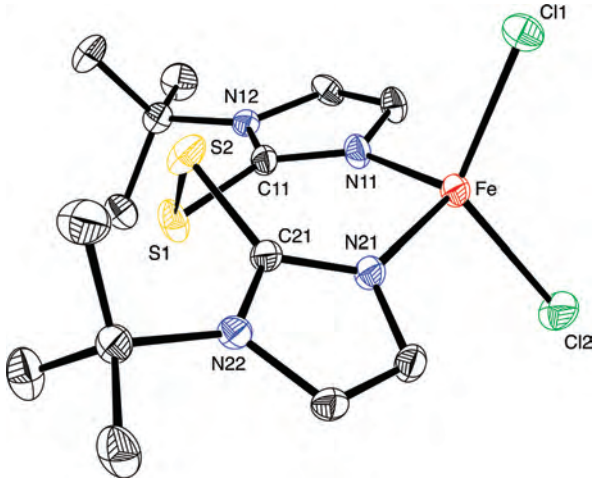

Figure 5. Molecular structure of $[\kappa^2\text{-}(mim^{But})_2]FeCl_2$.

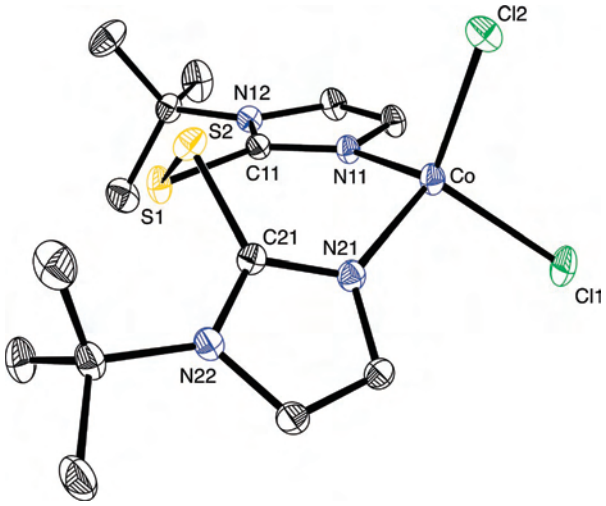

Figure 6. Molecular structure of $[\kappa^2\text{-}(mim^{But})_2]CoCl_2$.

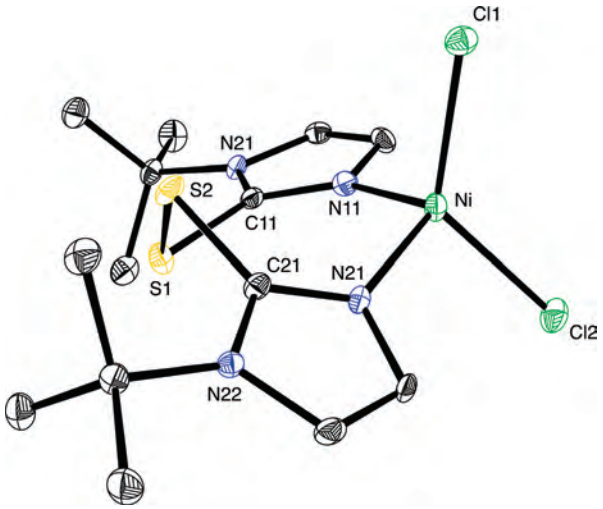

Figure 7. Molecular structure of $[\kappa^2\text{-}(mim^{But})_2]NiCl_2$.

of metal dichlorides, namely, $FeCl_2$, $CoCl_2$, $NiCl_2$, and $ZnCl_2$, giving rise to four-coordinate compounds of the type $[\kappa^2\text{-}(mim^R)_2]MCl_2$ (Scheme 2). The molecular structures of $[\kappa^2\text{-}(mim^{But})_2]MCl_2$ (M = Fe, Co, Ni, Zn) and $[\kappa^2\text{-}(mim^{Ph})_2]CoCl_2$ have been determined by X-ray diffraction, as illustrated in Figures 5−9, with selected metrical data presented in Tables

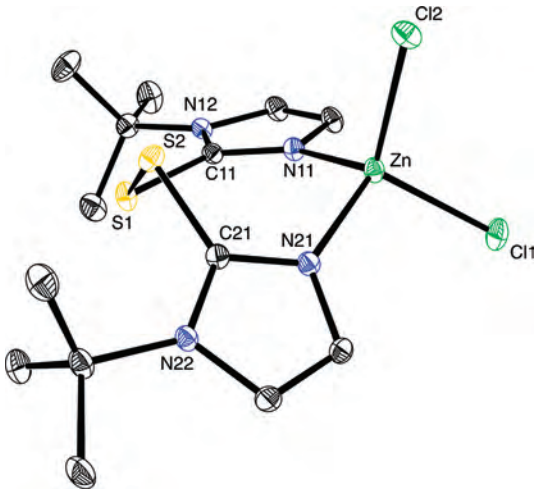

Figure 8. Molecular structure of $[\kappa^2\text{-}(\text{mim}^{\text{But}})_2]ZnCl_2$.

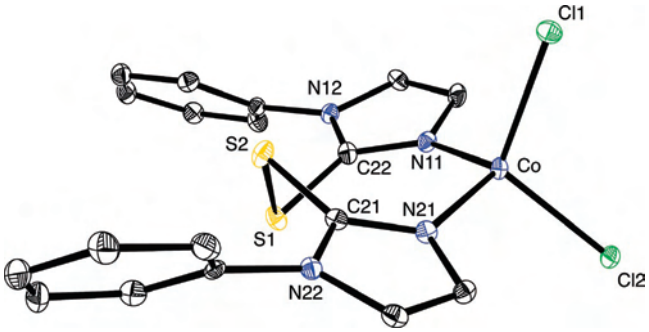

Figure 9. Molecular structure of $[\kappa^2\text{-}(\text{mim}^{\text{Ph}})_2]CoCl_2$.

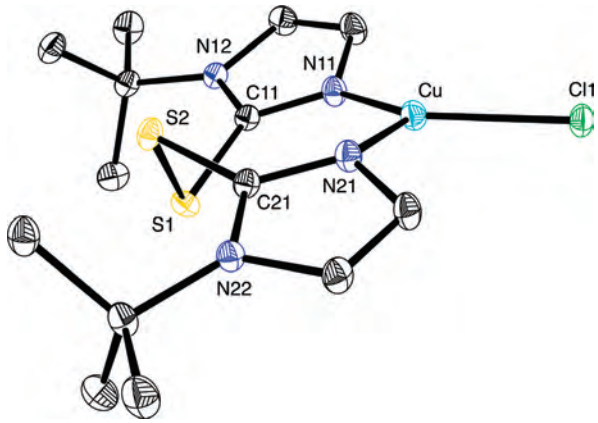

Figure 10. Molecular structure of $[\kappa^2\text{-}(\text{mim}^{\text{But}})_2]CuCl$.

2 and 3. Evaluation of the bond angles and the τ_4 four-coordinate geometry index[14] indicates that distortions from idealized tetrahedral geometry (with $\tau_4 = 1$) are greatest for the nickel and iron complexes, $[\kappa^2\text{-}(\text{mim}^{\text{But}})_2]NiCl_2$ ($\tau_4 = 0.87$) and $[\kappa^2\text{-}(\text{mim}^{\text{But}})_2]FeCl_2$ ($\tau_4 = 0.90$). It is also pertinent to note that, in each complex, the $[\kappa^2\text{-}(\text{mim}^{\text{R}})_2]$ ligands adopt a conformation in which the C−S−S−C torsion angles are approximately 90°, similar to that observed for the uncoordinated ligands.

In addition to four-coordinate $[\kappa^2\text{-}(\text{mim}^{\text{R}})_2]MCl_2$ complexes, three-coordinate copper(I) compounds $[\kappa^2\text{-}(\text{mim}^{\text{But}})_2]$-CuX (X = Cl, I) have also been isolated (Scheme 2) and structurally characterized by X-ray diffraction (Figures 10 and 11), with selected bond lengths and angles being listed in Tables 4 and 5. Copper(I) complexes with trigonal-planar geometries are less prevalent than tetrahedral derivatives;[15] the observation that $[\kappa^2\text{-}(\text{mim}^{\text{But}})_2]CuX$ exists as a three-coordinate monomer rather than a halide-bridged dimer is, therefore, noteworthy, especially so because $(\text{mim}^{\text{But}})_2$ is not a sterically demanding ligand.

An interesting aspect of ergothioneine disulfide is that it is less readily accessible via oxidation than are the corresponding disulfides derived from ovothiols.[6] A corollary of this observation is that the S−S bond of ergothioneine disulfide and $(\text{mim}^{\text{R}})_2$ should be subject to facile cleavage. In this regard, a common reaction of organodisulfides, R_2S_2, is cleavage of the S−S bond by oxidative addition to a low-valent metal center.[16] Such cleavage is not, however, observed for the above $[\kappa^2\text{-}(\text{mim}^{\text{R}})_2]MCl_2$ and $[\kappa^2\text{-}(\text{mim}^{\text{But}})_2]$-CuX complexes because access to M(IV) (M = Fe, Co, Ni) and Cu(III) is not typically a facile process in the absence of strongly electron-donating ancillary ligands. Therefore,

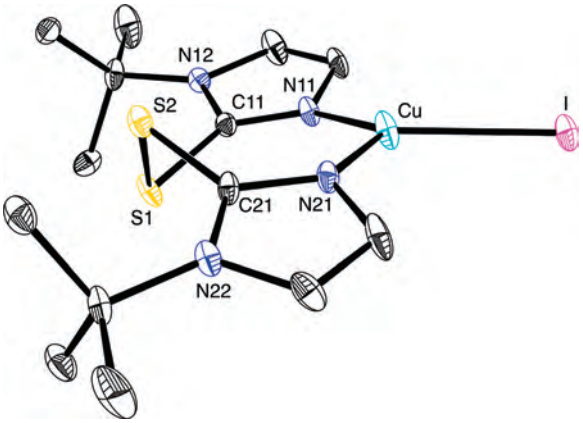

Figure 11. Molecular structure of $[\kappa^2\text{-}(\text{mim}^{\text{But}})_2]CuI$.

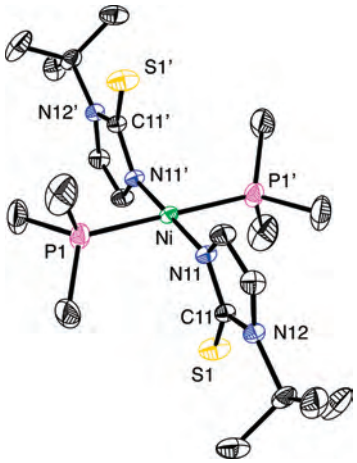

Figure 12. Molecular structure of *trans*-$Ni(PMe_3)_2(\text{mim}^{\text{But}})_2$.

(14) $\tau_4 = [360 - (\alpha + \beta)]/141$, where $\alpha + \beta$ is the sum of the two largest angles. See: Yang, L.; Powell, D. R.; Houser, R. P. *Dalton Trans.* **2007**, 955−964.

(15) (a) Batsanov, A. S.; Begley, M. J.; George, M. W.; Hubberstey, P.; Munakata, M.; Russell, C. E.; Walton, P. H. *Dalton Trans.* **1999**, 4251−4259 and references cited therein. (b) Eller, P. G.; Bradley, D. C.; Hursthouse, M. B.; Meek, D. W. *Coord. Chem. Rev.* **1977**, *24*, 1−95. (c) Smith, D. R. *Coord. Chem. Rev.* **1998**, *172*, 457−573.

(16) See, for example: Gonzales, J. M.; Musaev, D. J.; Morokuma, K. *Organometallics* **2005**, *24*, 4908−4914.

Table 2. Selected Bond Lengths (Å) for $[\kappa^2\text{-}(\text{mim}^{\text{R}})_2]\text{MCl}_2$ and $[\kappa^2\text{-}(\text{seim}^{\text{Mes}})_2]\text{MCl}_2$

	M−N11	M−N21	M−Cl1	M−Cl2	E1−E2	E1−C11	E2−C21
$[\kappa^2\text{-}(\text{mim}^{\text{But}})_2]\text{FeCl}_2$	2.060(4)	2.060(4)	2.262(2)	2.263(2)	2.076(3)	1.761(5)	1.749(5)
$[\kappa^2\text{-}(\text{mim}^{\text{But}})_2]\text{CoCl}_2$	2.031(3)	2.031(3)	2.282(1)	2.252(1)	2.056(1)	1.764(3)	1.757(3)
$[\kappa^2\text{-}(\text{mim}^{\text{Ph}})_2]\text{CoCl}_2$	2.028(8)	2.030(8)	2.255(3)	2.254(2)	2.081(3)	1.753(9)	1.748(9)
$[\kappa^2\text{-}(\text{mim}^{\text{But}})_2]\text{NiCl}_2$	1.987(3)	1.973(3)	2.241(1)	2.242(1)	2.063(2)	1.760(4)	1.760(4)
$[\kappa^2\text{-}(\text{mim}^{\text{But}})_2]\text{ZnCl}_2$	2.039(2)	2.007(2)	2.252(1)	2.250(1)	2.055(1)	1.766(3)	1.750(3)
$[\kappa^2\text{-}(\text{seim}^{\text{Mes}})_2]\text{FeCl}_2$	2.109(3)	2.088(3)	2.267(1)	2.255(1)	2.312(1)	1.904(4)	1.891(4)
$[\kappa^2\text{-}(\text{seim}^{\text{Mes}})_2]\text{CoCl}_2$	2.025(2)	2.025(2)	2.253(1)	2.253(1)	2.3284(6)	1.907(3)	1.907(3)
$[\kappa^2\text{-}(\text{seim}^{\text{Mes}})_2]\text{NiCl}_2$	2.014(4)	1.993(4)	2.246(1)	2.223(2)	2.3134(8)	1.905(5)	1.894(5)

Table 3. Selected Bond Angles (deg) for $[\kappa^2\text{-}(\text{mim}^{\text{R}})_2]\text{MCl}_2$ and $[\kappa^2\text{-}(\text{seim}^{\text{Mes}})_2]\text{MCl}_2$

	N11−M−N21	Cl1−M−Cl2	N11−M−Cl1	N21−M−Cl2	N11−M−Cl2	N21−M−Cl1	τ_4
$[\kappa^2\text{-}(\text{mim}^{\text{But}})_2]\text{FeCl}_2$	108.0(2)	120.42(7)	104.0(1)	103.2(1)	108.3(1)	112.5(1)	0.90
$[\kappa^2\text{-}(\text{mim}^{\text{But}})_2]\text{CoCl}_2$	107.5(1)	111.44(4)	107.81(8)	112.37(8)	112.37(8)	106.74(8)	0.96
$[\kappa^2\text{-}(\text{mim}^{\text{Ph}})_2]\text{CoCl}_2$	112.0(3)	111.4(1)	103.8(2)	107.3(2)	111.6(2)	110.8(2)	0.97
$[\kappa^2\text{-}(\text{mim}^{\text{But}})_2]\text{NiCl}_2$	108.3(1)	127.66(4)	102.8(1)	100.9(1)	106.2(1)	110.0(1)	0.87
$[\kappa^2\text{-}(\text{mim}^{\text{But}})_2]\text{ZnCl}_2$	106.56(9)	112.23(3)	107.49(6)	110.55(7)	111.69(7)	108.07(7)	0.97
$[\kappa^2\text{-}(\text{seim}^{\text{Mes}})_2]\text{FeCl}_2$	107.5(1)	120.72(5)	103.8(1)	108.1(1)	110.5(1)	105.5(1)	0.91
$[\kappa^2\text{-}(\text{seim}^{\text{Mes}})_2]\text{CoCl}_2$[a]	112.4(1)	114.43(5)	112.94(7)	112.94(7)	102.29(7)	102.29(7)	0.94
$[\kappa^2\text{-}(\text{seim}^{\text{Mes}})_2]\text{NiCl}_2$	105.7(2)	124.72(6)	100.3(1)	109.8(1)	111.4(1)	103.1(1)	0.89

[a] $[\kappa^2\text{-}(\text{seim}^{\text{Mes}})_2]\text{CoCl}_2$ resides on a crystallographic two-fold site and so Cl1/Cl2 and N11/N21 are symmetry-equivalent pairs in this case.

Table 4. Selected Bond Lengths (Å) for $[\kappa^2\text{-}(\text{mim}^{\text{But}})_2]\text{CuX}$ (X = Cl, I)

	Cu−N11	Cu−N21	Cu−X	S1−S2	S1−C11	S2−C21
$[\kappa^2\text{-}(\text{mim}^{\text{But}})_2]\text{CuCl}$	1.950(2)	2.038(2)	2.2390(7)	2.0708(8)	1.749(2)	1.754(2)
$[\kappa^2\text{-}(\text{mim}^{\text{But}})_2]\text{CuI}$	2.014(14)	1.970(14)	2.533(2)	2.070(6)	1.755(15)	1.765(17)

Table 5. Selected Bond Angles (deg) for $[\kappa^2\text{-}(\text{mim}^{\text{But}})_2]\text{CuX}$ (X = Cl, I)

	N11−Cu−N21	N11−Cu−X	N21−Cu−X
$[\kappa^2\text{-}(\text{mim}^{\text{But}})_2]\text{CuCl}$	120.91(8)	131.39(6)	107.60(6)
$[\kappa^2\text{-}(\text{mim}^{\text{But}})_2]\text{CuI}$	120.9(5)	121.9(4)	116.1(4)

in an endeavor to effect cleavage of the S−S bond, the reactivity of $(\text{mim}^{\text{But}})_2$ towards the electron-rich nickel(0) complex $\text{Ni(PMe}_3)_4$[17] was investigated.[18] $\text{Ni(PMe}_3)_4$ is indeed reactive towards $(\text{mim}^{\text{But}})_2$ and yields the square-planar *trans*-$\text{Ni(PMe}_3)_2(\text{mim}^{\text{But}})_2$ complex at room temperature (Scheme 3).

The most interesting aspect of *trans*-$\text{Ni(PMe}_3)_2(\text{mim}^{\text{But}})_2$ is concerned with the fact that the $(\text{mim}^{\text{But}})$ ligands coordinate only via their nitrogen atoms (Figure 12). This is a most uncommon coordination mode for mercaptoimidazolyl ligands, which typically coordinate either via sulfur alone or via both sulfur and nitrogen.[19] We are aware of only one complex that features unidentate nitrogen coordination of a mercaptoimidazolyl ligand, namely, the tin complex $\text{SnPh}_2[\text{C}_6\text{H}_3(\text{CH}_2\text{-OBu}^{\text{t}})_2](\text{mim}^{\text{Me}})$.[20]

The observation that the $(\text{mim}^{\text{But}})$ ligand coordinates via the nitrogen atom indicates that *trans*-$\text{Ni(PMe}_3)_2(\text{mim}^{\text{But}})_2$ is not simply formed by oxidative addition of the S−S bond because such a mechanism would yield the S-coordinated isomer; an additional step, therefore, involving rearrangement of the $(\text{mim}^{\text{But}})$ ligand would be required to give the observed product in which the nitrogen becomes the ligating atom. Density functional theory (DFT) calculations indicate that the N-coordinated isomer is 8.63 kcal mol^{-1} more stable than the S-coordinated isomer, and so it is feasible that the S-coordinated isomer could be the kinetic product, which rearranges to the N-coordinated thermodynamic product.[21]

An alternative mechanistic possibility, however, which is suggested by the fact that $(\text{mim}^{\text{But}})_2$ coordinates to MX_2 via the nitrogen atoms, is that formation of *trans*-$\text{Ni(PMe}_3)_2(\kappa^1\text{-mim}^{\text{But}})_2$ proceeds via a tetrahedral $[\kappa^2\text{-}(\text{mim}^{\text{But}})_2]\text{Ni(PMe}_3)_2$ intermediate in which $(\text{mim}^{\text{But}})_2$ coordinates initially by two of its nitrogen atoms and that S−S bond scission results from subsequent electron transfer from the nickel center through the ligand framework (Scheme 4).[22] In this regard, the disulfide $(\text{mim}^{\text{But}})_2$ may be viewed as a noninnocent ligand and the pair of $\{[\kappa^2\text{-}(\text{mim}^{\text{But}})_2]\text{M}\}$ and $\{[\kappa^1\text{-}(\text{mim}^{\text{But}})]_2\text{M}\}$ moieties may be viewed as redox isomers of each other.[23] Thus, it is possible that cleavage of the S−S bond could occur without requiring a direct Ni−S interaction.

(17) Klein, H.-F.; Schmidbaur, H. *Angew. Chem., Int. Ed. Engl.* **1970**, *9*, 903−904.

(18) Nickel thiolates are well precedented. See, for example, ref 3 and the following: (a) Maroney, M. J. *Curr. Opin. Chem. Biol.* **1999**, *3*, 188−199. (b) Eichhorn, D. M.; Goswami, N. *Comments Inorg. Chem.* **2003**, *24*, 1−13.

(19) (a) Miranda-Soto, V.; Pérez-Torrente, J. J.; Oro, L. A.; Lahoz, F. J.; Martin, M. L.; Parra-Hake, M.; Grotjahn, D. B. *Organometallics* **2006**, *25*, 4374−4390 and references cited therein. (b) Casas, J. S.; Castiñeiras, A.; Martínez, E. G.; González, A. S.; Sánchez, A.; Sordo, J. *Polyhedron* **1997**, *16*, 795−800. (c) Azam, K. A.; Hanif, K. M.; Ghosh, A. C.; Kabir, S. E.; Karmakar, S. R.; Malik, K. M. A.; Parvin, S.; Rosenberg, E. *Polyhedron* **2002**, *21*, 885−892. (d) Bonati, F.; Burini, A.; Pietroni, B. R.; Giorgini, E.; Bovio, B. *J. Organomet. Chem.* **1988**, *344*, 119−135. (e) Yap, G. P. A.; Jensen, C. M. *Inorg. Chem.* **1992**, *31*, 4823−4828. (f) Landgrafe, C.; Sheldrick, W. S.; Südfeld, M. *Eur. J. Inorg. Chem.* **1998**, 407−414.

(20) Martincová, J.; Dostál, L.; Taraba, J.; Jambor, R. *J. Organomet. Chem.* **2007**, *692*, 908−911.

(21) Experimental support that the N-coordinated isomer is thermodynamically more stable than the S-coordinated isomer is provided by the observation that *trans*-$\text{Ni(PMe}_3)_2(\kappa^1\text{-mim}^{\text{But}})_2$ retains its integrity in solution for extended periods at elevated temperature (ca. 75 °C, 3 days).

(22) The reaction has been monitored by NMR spectroscopy, but intermediates were not identified; as such, we have no evidence to distinguish these mechanistic possibilities.

Scheme 3

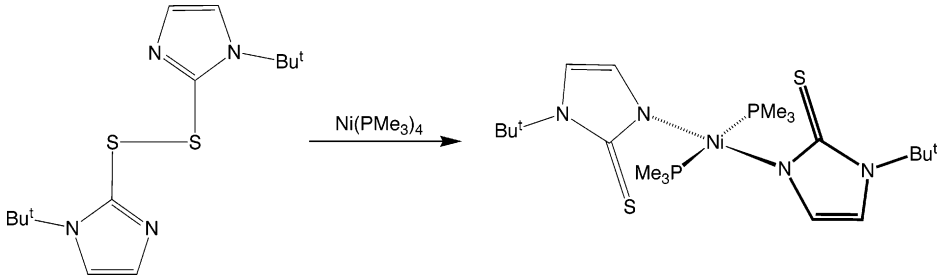

Scheme 4

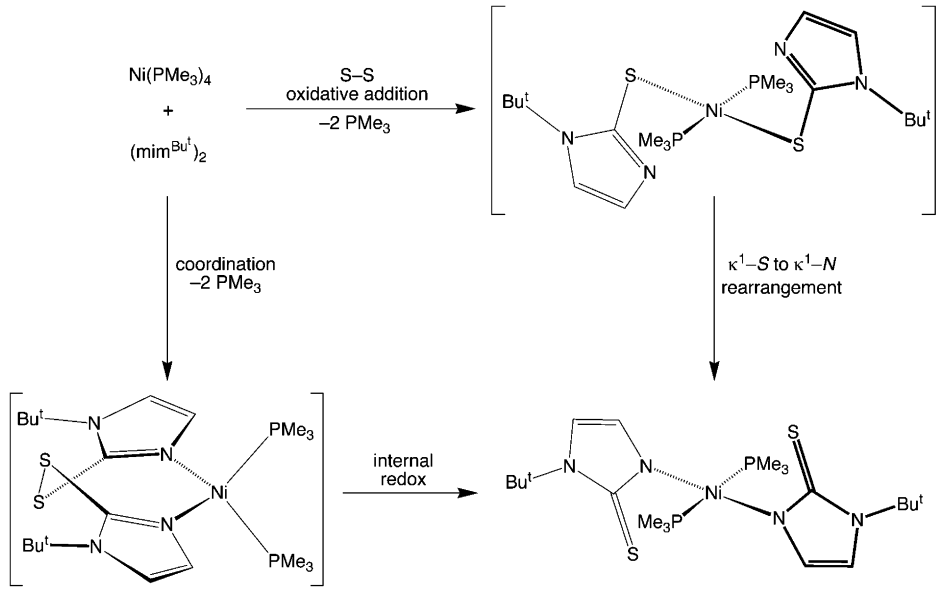

Scheme 5

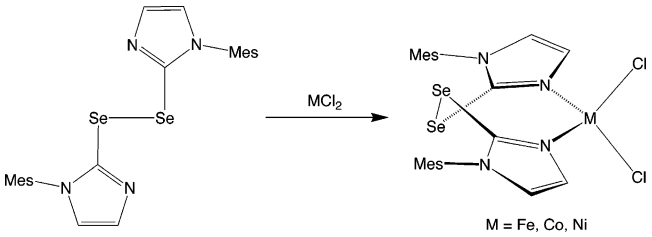

2. Bis(1-mesitylimidazol-2-yl)diselenide Complexes of Iron, Cobalt, and Nickel. In view of the above success of applying $(mim^R)_2$ as a bidentate ligand, we were prompted to evaluate the potential of the diselenide counterparts, and specifically the bis(1-mesitylimidazol-2-yl)diselenide derivative, $(seim^{Mes})_2$, that we have recently reported.[24] Indeed, the diselenide complexes $[\kappa^2\text{-}(seim^{Mes})_2]MCl_2$ (M = Fe, Co, Ni) may be readily obtained via treatment of $(seim^{Mes})_2$ with the corresponding metal dichloride (Scheme 5).[25] The molecular structures of $[\kappa^2\text{-}(seim^{Mes})_2]MCl_2$ have been determined by X-ray diffraction, as illustrated in Figures 13−15. Selected metrical data are listed in Tables 2 and 3, and the overall features are similar to those of the corresponding $[\kappa^2\text{-}(mim^R)_2]MCl_2$ derivatives, with the nickel complex (τ_4 = 0.89) showing the greatest deviation from tetrahedral geometry.

3. S−S/E−E (E = S, Se) Bond Metathesis Reactions of Bis(1-R-imidazol-2-yl)disulfide and Bis(1-mesitylimidazol-2-yl)diselenide Ligands. Each of the $\{[\kappa^2\text{-}(mim^R)_2]M\}$ and $\{[\kappa^2\text{-}(seim^{Mes})_2]M\}$ complexes described above contain ligands with *symmetric* disulfide and diselenide bridges. In order to increase the diversity of this class of molecules, we

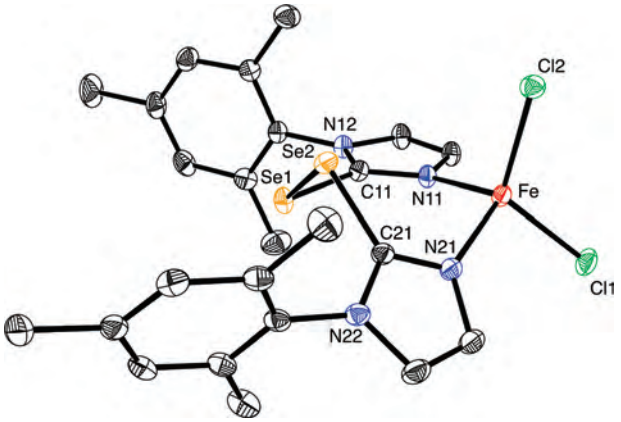

Figure 13. Molecular structure of $[\kappa^2\text{-}(seim^{Mes})_2]FeCl_2$.

(23) (a) Ray, K.; Petrenko, T.; Wieghardt, K.; Neese, F. *Dalton Trans.* **2007**, 1552−1566. (b) Evangelio, E.; Ruiz-Molina, D. *Eur. J. Inorg. Chem.* **2005**, 2957−2971. (c) Butin, K. P.; Beloglazkina, E. K.; Zyk, N. V. *Russ. Chem. Rev.* **2005**, *74*, 531−553. (d) Hendrickson, D. N.; Pierpont, C. G. *Top. Curr. Chem.* **2004**, *234*, 63−95. (e) Pierpont, C. G. *Coord. Chem. Rev.* **2001**, *219*−*221*, 415−433. (f) Pierpont, C. G. *Coord. Chem. Rev.* **2001**, *216*−*217*, 99−125. (g) Hirao, T. *Coord. Chem. Rev.* **2002**, *226*, 81−91. (h) Gütlich, P.; Dei, A. *Angew. Chem., Int. Ed. Engl.* **1997**, *36*, 2734−2737. (i) Zanello, P.; Corsini, M. *Coord. Chem. Rev.* **2006**, *250*, 2000−2022.

(24) Landry, V. K.; Minoura, M.; Pang, K.; Buccella, D.; Kelly, B. V.; Parkin, G. *J. Am. Chem. Soc.* **2006**, *128*, 12490−12497.

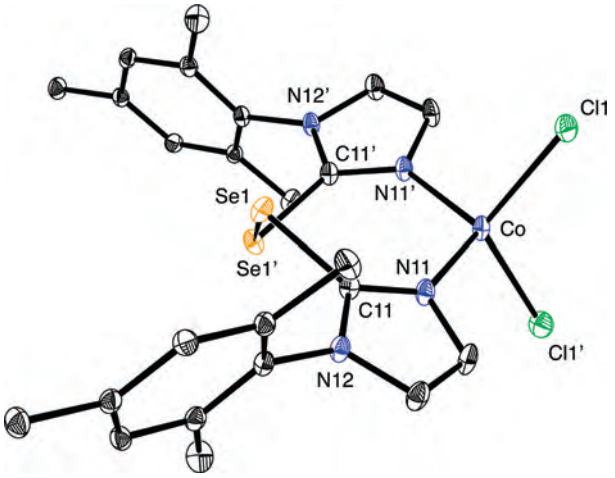

Figure 14. Molecular structure of $[\kappa^2\text{-}(\text{seim}^{\text{Mes}})_2]\text{CoCl}_2$.

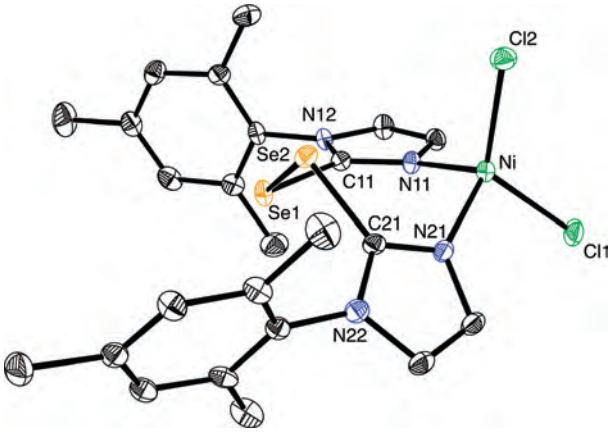

Figure 15. Molecular structure of $[\kappa^2\text{-}(\text{seim}^{\text{Mes}})_2]\text{NiCl}_2$.

Scheme 6

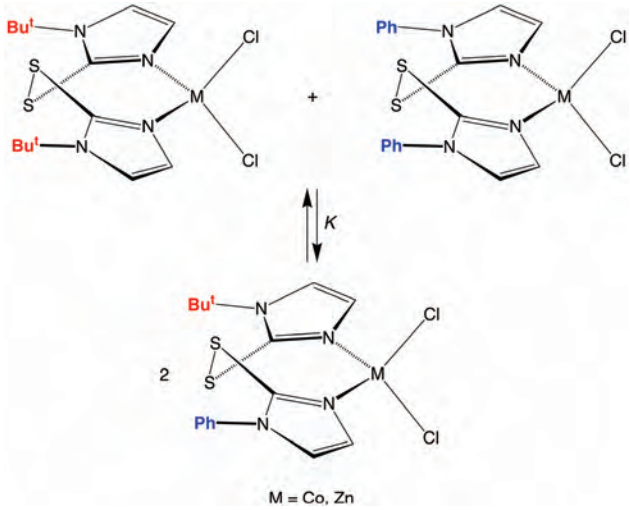

sought to synthesize variants with asymmetric bridges. It is, therefore, significant that a solution of $[\kappa^2\text{-}(\text{mim}^{\text{Ph}})_2]\text{CoCl}_2$ and $[\kappa^2\text{-}(\text{mim}^{\text{But}})_2]\text{CoCl}_2$ in $CDCl_3$ results in the rapid formation of an equilibrium mixture with the asymmetric disulfide $[\kappa^2\text{-}(\text{mim}^{\text{Ph}})(\text{mim}^{\text{But}})]\text{CoCl}_2$ (Scheme 6). Similarly, the zinc complexes, $[\kappa^2\text{-}(\text{mim}^{\text{Ph}})_2]\text{ZnCl}_2$ and $[\kappa^2\text{-}(\text{mim}^{\text{But}})_2]\text{-}\text{ZnCl}_2$, also undergo redistribution of the (mim^{R}) groups to form an equilibrium mixture with the asymmetric disulfide

Table 6. Equilibrium Constant Data for S−S and S−Se Metathesis (M = $CoCl_2$)

T/°C	K for $\{[\kappa^2\text{-}(\text{mim}^{\text{Ph}})_2]\text{M}\} + \{[\kappa^2\text{-}(\text{mim}^{\text{But}})_2]\text{M}\} \rightleftarrows 2\{[\kappa^2\text{-}(\text{mim}^{\text{Ph}})(\text{mim}^{\text{But}})]\text{M}\}$	K for $\{[\kappa^2\text{-}(\text{mim}^{\text{But}})_2]\text{M}\} + \{[\kappa^2\text{-}(\text{seim}^{\text{Mes}})_2]\text{M}\} \rightleftarrows 2\{[\kappa^2\text{-}(\text{mim}^{\text{But}})(\text{seim}^{\text{Mes}})]\text{M}\}$
0	6.61(47)	0.98(3)
30	6.46(15)	1.06(4)
40	6.14(12)	1.09(4)
50	−	1.13(4)
55	5.97(42)	−

Scheme 7

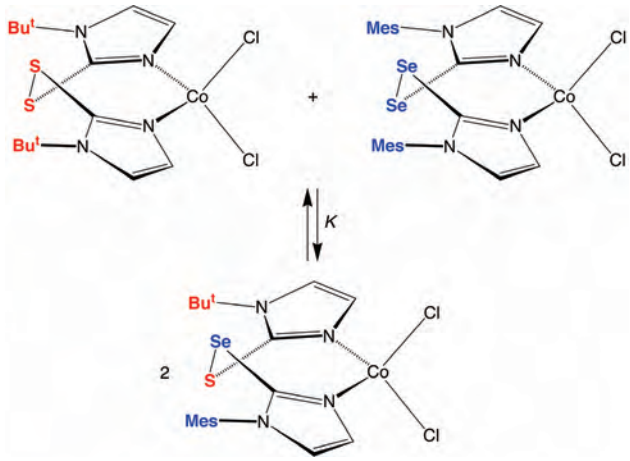

$[\kappa^2\text{-}(\text{mim}^{\text{Ph}})(\text{mim}^{\text{But}})]\text{ZnCl}_2$. The temperature dependence of the equilibrium constant for the cobalt system (Table 6) indicates that the reaction is almost thermoneutral, with $\Delta H = -0.3(1)$ kcal mol^{-1} and $\Delta S = 1.3(2)$ eu. If the enthalpy of the reaction is considered to be mainly associated with differences in the S−S bond enthalpies of the $[\kappa^2\text{-}(\text{mim}^{\text{Ph}})_2]$, $[\kappa^2\text{-}(\text{mim}^{\text{But}})_2]$, and $[\kappa^2\text{-}(\text{mim}^{\text{Ph}})(\text{mim}^{\text{But}})]$ ligands, the derived value of ΔH indicates that the S−S bond enthalpy of the mixed ligand $[\kappa^2\text{-}(\text{mim}^{\text{Ph}})(\text{mim}^{\text{But}})]$ is only ca. 0.15 kcal mol^{-1} more than the average of the S−S bond enthalpies of the $[\kappa^2\text{-}(\text{mim}^{\text{Ph}})_2]$ and $[\kappa^2\text{-}(\text{mim}^{\text{But}})_2]$ ligands.

In addition to metathesis involving two disulfide ligands, metathesis between disulfide and diselenide ligands has also been observed. Specifically, $[\kappa^2\text{-}(\text{mim}^{\text{But}})_2]\text{CoCl}_2$ and $[\kappa^2\text{-}(\text{seim}^{\text{Mes}})_2]\text{CoCl}_2$ undergo facile exchange to generate an equilibrium mixture with $[\kappa^2\text{-}(\text{mim}^{\text{But}})(\text{seim}^{\text{Mes}})]\text{CoCl}_2$ (Scheme 7). The temperature dependence of the equilibrium constant (Table 6) affords $\Delta H = 0.4(1)$ kcal mol^{-1} and $\Delta S = 1.6(1)$ eu. Assuming that the enthalpy of the reaction is largely determined by differences in S−S, Se−Se, and S−Se bond enthalpies, the S−Se bond enthalpy is 0.2 kcal mol^{-1} less than the average of the corresponding S−S and Se−Se bond energies. For comparison purposes, there is relatively little information pertaining to experimental E−E bond enthalpies, although the PhE−EPh bond enthalpies have recently been reported to be 46 (E = S), 41 (E = Se), and 33 (E = Te) kcal mol^{-1}.[26]

While the mechanisms of the metathesis reactions are unknown, the observation that the zinc complexes also

(25) It is worth noting that the reaction of $(\text{seim}^{\text{Me}})_2$ with $Cu(ClO_4)_2$ results in deselenation and the formation of $[(\kappa^2\text{-Se}(\text{mim}^{\text{Me}})_2\}\text{Cu}(\text{OH}_2)_2]\text{-}[\text{ClO}_4]_2$. See: Roy, G.; Nethaji, M.; Mugesh, G. *Inorg. Chem. Commun.* **2006**, *9*, 571−574.

undergo facile redistribution indicates that the exchange does not proceed via a process in which the S−S and Se−Se bonds are cleaved due to a redox process involving the metal. A variety of different possible mechanisms exist, and it is possible that trace quantities of $(mim^R)H$ or $(seim^R)H$ serve as a catalyst. In this regard, we have recently demonstrated that the $(seim^R)$ groups of the selone $(seim^R)H$ and diselenide $(seim^R)_2$ undergo exchange that is facile on the NMR time scale.[24] Furthermore, thiol/disulfide exchange,[27] thiol/diselenide exchange,[28] and selenol/diselenide exchange[29] is well precedented. Evidence that trace quantities of $(mim^R)H$ could serve as a catalyst for the exchange is provided by the observation that treatment of $[\kappa^2\text{-}(mim^{Bu^t})_2]CoCl_2$ with $(mim^{Ph})H$ rapidly gives an equilibrium mixture composed of $[\kappa^2\text{-}(mim^{Bu^t})_2]CoCl_2$, $[\kappa^2\text{-}(mim^{Ph})_2]CoCl_2$, $[\kappa^2\text{-}(mim^{Bu^t})(mim^{Ph})]CoCl_2$, $(mim^{Ph})H$, and $(mim^{Bu^t})H$.

Conclusions

Bis(1-R-imidazol-2-yl)disulfides and diselenides are useful bidentate (κ^2-N,N)-donor ligands for main-group and transition metals, as illustrated by the formation of $[\kappa^2\text{-}(mim^{Bu^t})_2]MCl_2$ (M = Fe, Co, Ni, Zn), $[\kappa^2\text{-}(mim^{Ph})_2]CoCl_2$, $[\kappa^2\text{-}(mim^{Bu^t})_2]CuX$ (X = Cl, I) and $[\kappa^2\text{-}(seim^{Mes})_2]MCl_2$ (M = Fe, Co, Ni) upon treatment of $(mim^R)_2$ or $(seim^{Mes})_2$ with the respective metal halide. However, if the metal center is capable of accessing a higher valence state, a redox transformation involving cleavage of the E−E bond becomes possible. Thus, the zerovalent nickel complex $Ni(PMe_3)_4$ effects cleavage of the disulfide bond of $(mim^{Bu^t})_2$ to give the square-planar complex *trans*-$Ni(PMe_3)_2(mim^{Bu^t})_2$. X-ray diffraction studies demonstrate that the (mim^{Bu^t}) ligands of *trans*-$Ni(PMe_3)_2(mim^{Bu^t})_2$ coordinate via nitrogen rather than sulfur; as such, the complex is not simply the result of oxidative addition of the S−S bond to the nickel center. While the observed isomer could be a result of ligand rearrangement, another possibility is that the formation of *trans*-$Ni(PMe_3)_2(\kappa^1\text{-}mim^{Bu^t})_2$ proceeds via a tetrahedral $[\kappa^2\text{-}(mim^{Bu^t})_2]Ni(PMe_3)_2$ intermediate in which $(mim^{Bu^t})_2$ coordinates initially by two of its nitrogen atoms and that S−S bond scission results from subsequent electron transfer from the nickel center through the ligand framework. Although $[\kappa^2\text{-}(mim^R)_2]MCl_2$ are not subject to homolytic cleavage of the S−S bond because the tetravalent state is not readily accessible, the observation that $[\kappa^2\text{-}(mim^{Ph})_2]CoCl_2$ and $[\kappa^2\text{-}(mim^{Bu^t})_2]CoCl_2$ form an equilibrium mixture with the asymmetric disulfide, $[\kappa^2\text{-}(mim^{Ph})(mim^{Bu^t})]CoCl_2$, indicates that S−S cleavage via another mechanism is possible. Likewise, metathesis between disulfide and diselenide ligands is observed in the formation of $[\kappa^2\text{-}(mim^{Bu^t})(seim^{Mes})]CoCl_2$ upon treatment of $[\kappa^2\text{-}(mim^{Bu^t})_2]CoCl_2$ with $[\kappa^2\text{-}(seim^{Mes})_2]CoCl_2$.

Experimental Section

General Considerations. All manipulations were performed using a combination of glovebox, high-vacuum, and Schlenk techniques under a nitrogen atmosphere unless otherwise specified.[30] Solvents were purified and degassed by standard procedures. ^1H NMR spectra were measured on Bruker 300 DRX, Bruker 400 DRX, and Bruker Avance 500 DMX spectrometers. ^1H NMR chemical shifts are reported in ppm relative to $SiMe_4$ ($\delta = 0$) and were referenced internally with respect to the protio solvent impurity (δ 7.16 for C_6D_5H;[31] δ 7.26 for $CHCl_3$). ^{31}P NMR chemical shifts are reported in ppm relative to 85% H_3PO_4 (δ 0) and were referenced using $P(OMe)_3$ (δ 141.0) as the external standard. Coupling constants are given in hertz. Mass spectra were obtained on a Micromass quadrupole-time-of-flight mass spectrometer using fast atom bombardment. Combustion analyses were carried out by Robertson Microlit Laboratories, Madison, NJ. $(mim^{Bu^t})H$,[10] $(mim^{Ph})H$,[12,32] $(seim^{Mes})_2$,[24] and $Ni(PMe_3)_4$[17] were prepared by literature methods.

Synthesis of $(mim^{Bu^t})_2$. I_2 (1.62 g, 6.4 mmol) was added in portions to a solution of $(mim^{Bu^t})H$ (2.00 g, 12.8 mmol) and NEt_3 (1.36 g, 13.4 mmol) in CH_2Cl_2 (100 mL). The resulting orange mixture was allowed to stir for an additional 30 min and then treated with H_2O (100 mL). The two layers were separated, and the CH_2Cl_2 layer was washed with H_2O (2 × 50 mL). The volatile components were removed in vacuo to give $(mim^{Bu^t})_2$ as an orange powder (1.79 g, 90%). ^1H NMR ($CDCl_3$): δ 7.10 [d, 2H, J = 1.5 Hz, Im], 7.06 [d, 2H, J = 1.5 Hz, Im], 1.52 [s, 18H, Bu^t]. IR (KBr, cm^{-1}): 3118(vs), 3102(vs), 2992(vs), 2970(vs), 2714(w), 2614(m), 2581(w), 2538(w), 2482(w), 2444(w), 2349(w), 2295(w), 1742(m), 1696(m), 1652(w), 1608(m), 1574(w), 1522(m), 1497(s), 1475(vs), 1420(vs), 1397(s), 1371(vs), 1365(vs), 1324(vs), 1292(m), 1249(vs), 1229(s), 1214(vs), 1193(s), 1155(s), 1138(s), 1120(vs), 1048(m), 1028(s), 932(w), 915(s), 849(w), 820(m), 787(vs), 763(vs), 693(vs), 593(s), 528(vs), 465(s), 447(m). Crystals suitable for X-ray diffraction were obtained from Et_2O.

Synthesis of $(mim^{Ph})_2$. I_2 (2.18 g, 8.60 mmol) was added in portions to a solution of $(mim^{Ph})H$ (3.05 g, 17.3 mmol) and NEt_3 (1.80 g, 17.7 mmol) in CH_2Cl_2 (100 mL). The resulting orange mixture was allowed to stir for an additional 30 min and then treated with H_2O (100 mL). The two layers were separated, and the CH_2Cl_2 layer was washed with H_2O (2 × 50 mL). The volatile components were removed in vacuo to give $(mim^{Ph})_2$ as an orange

(26) McDonough, J. E.; Weir, J. J.; Carlson, M. J.; Hoff, C. D.; Kryatova, O. P.; Rybak-Akimova, E. V.; Clough, C. R.; Cummins, C. C. *Inorg. Chem.* **2005**, *44*, 3127−3136.
(27) (a) Singh, R.; Whitesides, G. M. *J. Am. Chem. Soc.* **1990**, *112*, 1190−1197. (b) Singh, R.; Whitesides, G. M. *J. Org. Chem.* **1991**, *56*, 6931−6933. (c) Guo, W.; Pleasants, J.; Rabenstein, D. L. *J. Org. Chem.* **1990**, *55*, 373−376. (d) Fernandes, P. A.; Ramos, M. J. *Chem.−Eur. J.* **2004**, *10*, 257−266. (e) Lees, W. J.; Whitesides, G. M. *J. Org. Chem.* **1993**, *58*, 642−647. (f) Theriault, Y.: Cheesman, B. V.; Arnold, A. P.; Rabenstein, D. L. *Can. J. Chem.* **1984**, *62*, 1312−1319. (g) Theriault, Y.; Rabenstein, D. L. *Can. J. Chem.* **1985**, *63*, 2225−2231. (h) Rabenstein, D. L.; Theriault, Y. *Can. J. Chem.* **1984**, *62*, 1672−1680. (i) Keire, D. A.; Guo, W.; Rabenstein, D. L. *Magn. Reson. Chem.* **1992**, *30*, 746−753. (j) Rabenstein, D. L.; Theriault, Y. *Can. J. Chem.* **1985**, *63*, 33−39.
(28) Engman, L.; Stern, D. *J. Org. Chem.* **1994**, *59*, 5179−5183.
(29) (a) Tan, K.-S.; Arnold, A. P.; Rabenstein, D. L. *Can. J. Chem.* **1988**, *66*, 54−60. (b) Pleasants, J. C.; Guo, W.; Rabenstein, D. L. *J. Am. Chem. Soc.* **1989**, *111*, 6553−6558. (c) Reich, H. J.; Jasperse, C. P. *J. Am. Chem. Soc.* **1987**, *109*, 5549−5551.
(30) (a) McNally, J. P.; Leong, V. S.; Cooper, N. J. In *Experimental Organometallic Chemistry*; Wayda, A. L., Darensbourg, M. Y., Eds.; American Chemical Society: Washington, DC, 1987; Chapter 2, pp 6−23. (b) Burger, B.J.; Bercaw, J. E. In *Experimental Organometallic Chemistry*; Wayda, A. L., Darensbourg, M. Y., Eds.; American Chemical Society: Washington, DC, 1987; Chapter 4, pp 79−98. (c) Shriver, D. F.; Drezdzon, M. A. *The Manipulation of Air-Sensitive Compounds*, 2nd ed.; Wiley-Interscience: New York, 1986.
(31) Gottlieb, H. E.; Kotlyar, V.; Nudelman, A. *J. Org. Chem.* **1997**, *62*, 7512−7515.
(32) $(mim^{Ph})H$ was prepared using the method described in ref 10.

powder (2.54 g, 84%). ^{1}H NMR ($CDCl_3$): δ 7.40 [m, 6H, Ph], 7.22 [s, 2H, Im], 7.14 [m, 6H, Ph and Im]. IR (KBr, cm^{-1}): 3132-(m), 3115(m), 1716(w), 1652(w), 1595(m), 1558(w), 1539(vw), 1500(vs), 1487(s), 1455(m), 1426(vs), 1338(w), 1307(m), 1299-(s), 1263(w), 1173(w), 1159(m), 1123(s), 1092(m), 1085(m), 1074-(m), 1030(w), 1003(w), 980(w), 908(m), 870(w), 831(w), 782(s), 771(vs), 764(vs), 756(vs), 693(vs), 668(m), 639(w), 561(m), 493-(s), 482(m). Crystals suitable for X-ray diffraction were obtained from CH_2Cl_2.

Synthesis of [κ^2-(mim$^{Bu^t}$)$_2$]FeCl$_2$. A solution of (mim$^{Bu^t}$)$_2$ (0.600 g, 1.93 mmol) in CH_2Cl_2 (5 mL) was added to a slurry of $FeCl_2$ (0.275 g, 2.17 mmol) in CH_2Cl_2 (1 mL). The mixture was allowed to stir for 18 h and then filtered. The volatile components were removed from the filtrate in vacuo, and the resulting residue was extracted with CH_2Cl_2 (3 mL). The solution was placed at −35 °C, thereby depositing [κ^2-(mim$^{Bu^t}$)$_2$]$FeCl_2$ as orange crystals over a period of 3 days, which were isolated and dried in vacuo (0.264 g, 31%). ^{1}H NMR ($CDCl_3$, 300 MHz, 25 °C): δ 64.0 [s, 2H, Im], 47.5 [s, 2H, Im], 1.51 [s, 18H, Bu^t]. μ_{eff} (Evans method): 5.2 μ_B. Anal. Calcd for [κ^2-(mim$^{Bu^t}$)$_2$]$FeCl_2$: C, 38.5; H, 5.1; N, 12.8. Found: C, 38.2; H, 4.9; N, 12.6. Crystals suitable for X-ray diffraction were obtained from CH_2Cl_2.

Synthesis of [κ^2-(mim$^{Bu^t}$)$_2$]CoCl$_2$. A solution of (mim$^{Bu^t}$)$_2$ (0.500 g, 1.61 mmol) in CH_2Cl_2 (5 mL) was added to a slurry of $CoCl_2$ (0.234 g, 1.80 mmol) in CH_2Cl_2 (1 mL). The mixture was allowed to stir for 18 h and then filtered. The volatile components were removed from the filtrate in vacuo, and the resulting residue was extracted with CH_2Cl_2 (3 mL). The solution was placed at −35 °C, thereby depositing [κ^2-(mim$^{Bu^t}$)$_2$]$CoCl_2$ as blue crystals over a period of 3 days, which were isolated and dried in vacuo (0.313 g, 44%). ^{1}H NMR ($CDCl_3$): δ 71.9 [s, 2H, Im], 49.6 [s, 2H, Im], 2.92 [s, 18H, Bu^t]. μ_{eff} (Evans method): 4.4 μ_B. Anal. Calcd for [κ^2-(mim$^{Bu^t}$)$_2$]$CoCl_2$: C, 38.2; H, 5.0; N, 12.7. Found: C, 38.1; H, 5.0; N, 12.7. Crystals suitable for X-ray diffraction were obtained from CH_2Cl_2.

Synthesis of [κ^2-(mim$^{Bu^t}$)$_2$]NiCl$_2$. A solution of (mim$^{Bu^t}$)$_2$ (0.250 g, 0.80 mmol) in CH_2Cl_2 (3 mL) was added to a slurry of $NiCl_2$ (0.156 g, 1.20 mmol) in CH_2Cl_2 (1 mL). The mixture was allowed to stir for 18 h and then filtered. The volatile components were removed from the filtrate in vacuo, and the resulting residue was extracted with CH_2Cl_2 (1.5 mL). The solution was placed at −35 °C, thereby depositing [κ^2-(mim$^{Bu^t}$)$_2$]$NiCl_2$ as a purple precipitate over a period of 1 day, which was isolated and dried in vacuo (0.108 g, 31%). ^{1}H NMR ($CDCl_3$): δ 99.3 [s, 2H, Im], 61.7 [s, 2H, Im], 6.17 [s, 18H, Bu^t]. μ_{eff} (Evans method): 2.9 μ_B. MS: *m*/*z* 403.15 {M − Cl}$^+$. Crystals suitable for X-ray diffraction were obtained from CH_2Cl_2.

Synthesis of [κ^2-(mim$^{Bu^t}$)$_2$]ZnCl$_2$. A solution of (mim$^{Bu^t}$)$_2$ (0.300 g, 0.97 mmol) in CH_2Cl_2 (3 mL) was added to a slurry of $ZnCl_2$ (0.144 g, 1.06 mmol) in CH_2Cl_2 (1 mL). The mixture was allowed to stir for 18 h and then filtered. The volatile components were removed from the filtrate in vacuo, and the resulting residue was extracted with CH_2Cl_2 (2 mL). The solution was placed at −35 °C, thereby depositing [κ^2-(mim$^{Bu^t}$)$_2$]$ZnCl_2$ as pale-yellow crystals over a period of 3 days, which were isolated and dried in vacuo (0.086 g, 20%). ^{1}H NMR ($CDCl_3$): δ 7.55 [d, 2H, J = 1.5 Hz, Im], 7.27 [d, 2H, J = 1.5 Hz, Im], 1.72 [s, 18H, Bu^t]. Anal. Calcd for [κ^2-(mim$^{Bu^t}$)$_2$]$ZnCl_2$: C, 37.6; H, 5.0; N, 12.5. Found: C, 37.7; H, 4.7; N, 12.4. Crystals suitable for X-ray diffraction were obtained from CH_2Cl_2.

Synthesis of [κ^2-(mim^{Ph})$_2$]CoCl$_2$. A solution of (mim^{Ph})$_2$ (0.200 g, 0.57 mmol) in CH_2Cl_2 (3 mL) was added to a slurry of $CoCl_2$ (0.081 g, 0.62 mmol) in CH_2Cl_2 (1 mL). The mixture was allowed to stir for 18 h and then filtered. The volatile components were removed from the filtrate in vacuo, and the resulting residue was extracted with CH_2Cl_2 (3 mL). The solution was placed at −35 °C, thereby depositing [κ^2-(mim^{Ph})$_2$]$CoCl_2$ as blue crystals over a period of 2 days, which were isolated and dried in vacuo (0.198 g, 72%). ^{1}H NMR ($CDCl_3$): δ 63.7 [s, 2H, Im], 45.7 [s, 2H, Im], 8.11 [s, 4H, Ph], 6.18 [s, 2H, Ph], 5.95 [s, 4H, Ph]. Anal. Calcd for [κ^2-(mim^{Ph})$_2$]$CoCl_2$·CH_2Cl_2: C, 40.4; H, 2.9; N, 9.9. Found: C, 39.9; H, 2.4; N, 9.7. Crystals suitable for X-ray diffraction were obtained from CH_2Cl_2.

Synthesis of [κ^2-(mim^{Ph})$_2$]ZnCl$_2$. A solution of (mim^{Ph})$_2$ (0.300 g, 0.85 mmol) in CH_2Cl_2 (3 mL) was added to a slurry of $ZnCl_2$ (0.127 g, 0.94 mmol) in CH_2Cl_2 (1 mL). The mixture was allowed to stir for 18 h and then filtered. The volatile components were removed from the filtrate in vacuo, and the resulting residue was extracted with CH_2Cl_2 (2 mL). The solution was placed at −35 °C, thereby depositing [κ^2-(mim^{Ph})$_2$]$ZnCl_2$ as pale-yellow crystals over a period of 6 days, which were isolated and dried in vacuo (0.089 g, 22%). ^{1}H NMR ($CDCl_3$): δ 7.72 [s, 2H, Ph], 7.54 [s, 6H, Im and Ph], 7.35 [s, 2H, Im], 7.31 [s, 4H, Ph]. Anal. Calcd for [κ^2-(mim^{Ph})$_2$]$ZnCl_2$·CH_2Cl_2: C, 39.9; H, 2.8; N, 9.8. Found: C, 38.7; H, 2.8; N, 9.3.

Synthesis of [κ^2-(seim^{Mes})$_2$]FeCl$_2$. A solution of (seim^{Mes})$_2$ (0.200 g, 0.38 mmol) in CH_2Cl_2 (5 mL) was added to a slurry of $FeCl_2$ (0.048 g, 0.38 mmol) in CH_2Cl_2 (1 mL). The mixture was allowed to stir for 18 h and then filtered. The volatile components were removed from the filtrate in vacuo, and the resulting residue was extracted with CH_2Cl_2 (2 mL). The solution was placed at −35 °C, thereby depositing [κ^2-(seim^{Mes})$_2$]$FeCl_2$ as orange crystals over a period of 2 days, which were isolated and dried in vacuo (0.153 g, 62%). ^{1}H NMR ($CDCl_3$): δ 65.9 [s, 2H, Im], 42.9 [s, 2H, Im], 7.37 [s, 4H, *m*-Mes], 2.10 [s, 12H, *p*-CH_3Mes], 1.12 [s, 6H, *o*-CH_3Mes]. Anal. Calcd for [κ^2-(seim^{Mes})$_2$]$FeCl_2$: C, 44.0; H, 4.0; N, 8.6. Found: C, 43.0; H, 3.8; N, 8.3. MS: *m*/*z* 621.0 {M − Cl}$^+$. Crystals suitable for X-ray diffraction were obtained from CH_2Cl_2.

Synthesis of [κ^2-(seim^{Mes})$_2$]CoCl$_2$. A solution of (seim^{Mes})$_2$ (0.085 g, 0.16 mmol) in CH_2Cl_2 (3 mL) was added to a slurry of $CoCl_2$ (0.031 g, 0.24 mmol) in CH_2Cl_2 (1 mL). The mixture was allowed to stir for 18 h and then filtered. The volatile components were removed from the filtrate in vacuo, and the resulting residue was extracted with CH_2Cl_2 (2 mL). The solution was placed at −35 °C, thereby depositing [κ^2-(seim^{Mes})$_2$]$CoCl_2$ as green crystals over a period of 2 days, which were isolated and dried in vacuo (0.049 g, 47%). ^{1}H NMR ($CDCl_3$): δ 69.8 [s, 2H, Im], 44.6 [s, 2H, Im], 7.83 [s, 4H, *m*-Mes], 2.72 [s, 6H, *p*-CH_3Mes], 1.26 [br s, 12H, *o*-CH_3Mes]. MS: *m*/*z* 622.2 {M − Cl}$^+$. Crystals suitable for X-ray diffraction were obtained from CH_2Cl_2.

Synthesis of [κ^2-(seim^{Mes})$_2$]NiCl$_2$. A solution of (seim^{Mes})$_2$ (0.090 g, 0.17 mmol) in CH_2Cl_2 (5 mL) was added to a slurry of $NiCl_2$ (0.029 g, 0.22 mmol) in CH_2Cl_2 (1 mL). The mixture was allowed to stir for 30 h and then filtered. The volatile components were removed from the filtrate in vacuo, and the resulting residue was extracted with CH_2Cl_2 (2 mL). The solution was placed at −35 °C, thereby depositing [κ^2-(seim^{Mes})$_2$]$NiCl_2$ as green crystals over a period of 2 days, which were isolated and dried in vacuo (0.033 g, 30%). ^{1}H NMR ($CDCl_3$): δ 88.2 [s, 2H, Im], 54.4 [s, 2H, Im], 8.66 [s, 4H, *m*-Mes], 3.60 [s, 6H, *p*-CH_3Mes], 3.47 [s, 12H, *o*-CH_3Mes]. MS: *m*/*z* 623.1 {M − Cl}$^+$. Crystals suitable for X-ray diffraction were obtained from $CHCl_3$.

Synthesis of [κ^2-(mim$^{Bu^t}$)$_2$]CuCl. A solution of (mim$^{Bu^t}$)$_2$ (0.300 g, 0.96 mmol) in CH_2Cl_2 (3 mL) was added to a slurry of CuCl (0.100 g, 1.01 mmol) in CH_2Cl_2 (1 mL). The mixture was allowed

Table 7. Crystal, Intensity Collection and Refinement Data

	$(mim^{Bu^t})_2$	$(mim^{Ph})_2$	$[\kappa^2\text{-}(mim^{Bu^t})_2]\text{-}FeCl_2$	$[\kappa^2\text{-}(mim^{Bu^t})_2]\text{-}CoCl_2\cdot 2CH_2Cl_2$	$[\kappa^2\text{-}(mim^{Bu^t})_2]\text{-}NiCl_2\cdot CH_2Cl_2$
lattice	orthorhombic	monoclinic	monoclinic	monoclinic	orthorhombic
formula	$C_{14}H_{22}N_4S_2$	$C_{18}H_{14}N_4S_2$	$C_{23}H_{31}Cl_2FeN_4S_2$	$C_{16}H_{26}Cl_6CoN_4S_2$	$C_{15}H_{24}Cl_4N_4NiS_2$
fw	310.48	700.90	554.39	610.16	525.01
space group	*Pbca*	$P2_1/n$	$P2_1/c$	$P2_1/n$	*Pbca*
a/Å	13.0132(11)	12.9142(13)	12.415(5)	13.3552(13)	20.146(2)
b/Å	11.9125(10)	8.8002(9)	20.520(8)	14.3521(15)	10.620(1)
c/Å	21.4092(19)	14.5441(15)	10.938(5)	13.9868(14)	20.869(3)
α/deg	90	90	90	90	90
β/deg	90	91.9310(10)	94.253(7)	93.275(2)	90
γ/deg	90	90	90	90	90
V/Å^3	3318.8(5)	1652.0(3)	2779(2)	2676.5(5)	4465.1(9)
Z	8	4	4	4	8
T/K	243(2)	125(2)	243(2)	243(2)	125(2)
λ/Å	0.710 73	0.710 73	0.710 73	0.710 73	0.710 73
ρ(calcd)/g cm^{-3}	1.243	1.409	1.325	1.514	1.562
μ(Mo Kα)/mm^{-1}	0.317	0.329	0.903	1.408	1.543
R1	0.0435	0.0322	0.0512	0.0458	0.0378
wR2	0.0915	0.1165	0.1107	0.1154	0.0759

	$[\kappa^2\text{-}(mim^{Bu^t})_2]\text{-}CuCl\cdot CH_2Cl_2$	$[\kappa^2\text{-}(mim^{Bu^t})_2]\text{-}CuI$	$[\kappa^2\text{-}(mim^{Bu^t})_2]\text{-}ZnCl_2\cdot 2CH_2Cl_2$	$[\kappa^2\text{-}(mim^{Ph})_2]\text{-}CoCl_2\cdot CH_2Cl_2$
lattice	triclinic	triclinic	monoclinic	monoclinic
formula	$C_{15}H_{24}Cl_3CuN_4S_2$	$C_{14}H_{22}CuIN_4S_2$	$C_{16}H_{26}Cl_6N_4S_2Zn$	$C_{19}H_{16}Cl_4CoN_4S_2$
fw	494.39	500.92	616.60	565.21
space group	$P\bar{1}$	$P\bar{1}$	$P2_1/n$	$P2_1/c$
a/Å	9.6250(17)	9.2589(8)	13.1296(10)	6.7689(10)
b/Å	9.6646(18)	9.9669(9)	14.2593(11)	23.862(3)
c/Å	11.838(2)	10.8822(9)	13.9286(11)	14.198(2)
α/deg	100.645(3)	85.774(2)	90	90
β/deg	100.726(3)	89.877(2)	93.0420(10)	100.066(2)
γ/deg	91.950(3)	70.0330(10)	90	90
V/Å^3	1060.6(3)	941.02(14)	2604.0(3)	2257.9(6)
Z	2	2	4	4
T/K	243(2)	243(2)	125(2)	125(2)
λ/Å	0.710 73	0.710 73	0.710 73	0.710 73
ρ(calcd)/g cm^{-3}	1.548	1.768	1.573	1.663
μ(Mo Kα)/mm^{-1}	1.611	3.024	1.731	1.434
R1	0.0348	0.0785	0.0436	0.0814
wR2	0.1476	0.2216	0.0976	0.2265

	$[\kappa^2\text{-}(seim^{Mes})_2]\text{-}FeCl_2$	$[\kappa^2\text{-}(seim^{Mes})_2]\text{-}CoCl_2$	$[\kappa^2\text{-}(seim^{Mes})_2]\text{-}NiCl_2\cdot CHCl_3$	$Ni(PMe_3)_2\text{-}(\kappa^1\text{-}mim^{Bu^t})_2\cdot C_7H_8$
lattice	monoclinic	monoclinic	monoclinic	triclinic
formula	$C_{25}H_{28}Cl_4FeN_4Se_2$	$C_{24}H_{26}Cl_2CoN_4Se_2$	$C_{25}H_{27}Cl_5N_4NiSe_2$	$C_{27}H_{48}N_4NiP_2S_2$
fw	740.08	658.24	777.39	613.46
space group	$P2_1/n$	$C2/c$	$P2_1/n$	$P\bar{1}$
a/Å	8.6315(8)	23.968(3)	8.6691(8)	7.3358(14)
b/Å	14.2880(14)	8.1797(10)	14.2662(15)	9.3361(19)
c/Å	25.144(3)	16.2729(19)	25.323(3)	13.886(4)
α/deg	90	90	90	74.588(8)
β/deg	98.144(2)	124.719(2)	96.840(2)	84.137(14)
γ/deg	90	90	90	68.513(5)
V/Å^3	3069.7(5)	2622.3(5)	3109.6(5)	853.1(3)
Z	4	4	4	1
T/K	243(2)	243(2)	243(2)	243(2)
λ/Å	0.710 73	0.71073	0.71073	0.710 73
ρ(calcd)/g cm^{-3}	1.601	1.667	1.661	1.194
μ(Mo Kα)/mm^{-1}	3.232	3.654	3.417	0.806
R1	0.0392	0.0287	0.0484	0.0425
wR2	0.0829	0.0681	0.0786	0.1102

to stir for 18 h and then filtered. The volatile components were removed from the filtrate in vacuo, and the resulting residue was extracted with CH_2Cl_2 (2 mL). The solution was placed at −35 °C, thereby depositing $[\kappa^2\text{-}(mim^{Bu^t})_2]CuCl$ as orange crystals over a period of 3 days, which were isolated and dried in vacuo (0.238 g, 60%). ^{1}H NMR ($CDCl_3$): δ 7.51 [s, 2H, Im], 7.34 [s, 2H, Im], 1.72 [s, 18H, Bu^t]. Anal. Calcd for $[\kappa^2\text{-}(mim^{Bu^t})_2]CuCl\cdot CH_2Cl_2$: C, 36.4; H, 4.9; N, 11.3. Found: C, 36.5; H, 4.8; N, 11.3. Crystals suitable for X-ray diffraction were obtained from CH_2Cl_2.

Synthesis of $[\kappa^2\text{-}(mim^{Bu^t})_2]CuI$. A solution of $(mim^{Bu^t})_2$ (0.100 g, 0.32 mmol) in CH_2Cl_2 (2 mL) was added to a slurry of CuI (0.064 g, 0.34 mmol) in CH_2Cl_2 (1 mL). The mixture was allowed to stir for 18 h and then filtered. The volatile components were removed from the filtrate in vacuo, and the resulting residue was extracted with CH_2Cl_2 (2 mL). The solution was placed at

−35 °C, thereby depositing [κ^2-(mim$^{Bu^t}$)$_2$]CuI as orange crystals over a period of 2 days, which were isolated and dried in vacuo (0.030 g, 19%). ^{1}H NMR ($CDCl_3$): δ 7.44 [s, 2H, Im], 7.17 [s, 2H, Im], 1.70 [s, 18H, Bu^t]. MS: *m*/*z* 373.1 {M − I}$^+$. Crystals suitable for X-ray diffraction were obtained from CH_2Cl_2.

Synthesis of *trans*-Ni(mim$^{Bu^t}$)$_2$(PMe$_3$)$_2$. A solution of Ni(PMe$_3$)$_4$ (0.461 g, 1.27 mmol) in C_6H_6 (3 mL) was added to a solution of (mim$^{Bu^t}$)$_2$ (0.395 g, 1.27 mmol) in C_6H_6 (3 mL), and the mixture was stirred for 45 min at room temperature. After this period, the volatile components were removed in vacuo and the resulting orange residue was extracted into toluene (5 mL) and filtered. The filtrate was placed at −15 °C, thereby depositing orange crystals of *trans*-Ni(mim$^{Bu^t}$)$_2$(PMe$_3$)$_2$, over a period of 2 days, which were isolated and dried in vacuo (0.190 g, 29%). ^{1}H NMR (C_6D_6): δ 6.84 [s, 2H, Im], 6.47 [s, 2H, Im], 1.70 [s, 18H, Bu^t], 1.29 [s, 9H, PMe$_3$]. ^{31}P{^{1}H} NMR (C_6D_6): δ 32.7. Anal. Calcd for Ni(mim$^{Bu^t}$)$_2$-(PMe$_3$)$_2$: C, 46.1; H, 7.7; N, 10.8. Found: C, 48.2; H, 8.2; N, 10.1. Crystals suitable for X-ray diffraction were obtained from toluene.

S−S Bond Metathesis between [κ^2-(mim$^{Bu^t}$)$_2$]CoCl$_2$ and [κ^2-(mim^{Ph})$_2$]CoCl$_2$. A solution of [κ^2-(mim$^{Bu^t}$)$_2$]CoCl$_2$ (0.014 g, 0.032 mmol) in $CDCl_3$ (0.6 mL) containing Cp_2Fe (0.004 g, 0.022 mmol) as an internal standard was added to a solution of [κ^2-(mim^{Ph})$_2$]-CoCl$_2$ (0.016 g, 0.032 mmol) in $CDCl_3$ (0.5 mL). The mixture was transferred to a Teflon-capped NMR tube (J-Young) and monitored by ^{1}H NMR spectroscopy, thereby demonstrating that an equilibrium mixture with [κ^2-(mim^{Ph})(mim$^{Bu^t}$)]CoCl$_2$ was reached over a period of ca. 24 h at room temperature. ^{1}H NMR data for [κ^2-(mim^{Ph})(mim$^{Bu^t}$)]CoCl$_2$ ($CDCl_3$): δ 68.0 [s, 2H, Im], 55.1 [s, 1H, Im], 41.6 [s, 1H, Im], 8.19 [s, 2H, Ph], 6.32 [s, 3H, Ph], 2.81 [s, 9H, Bu^t]. The equilibrium constant for the formation of [κ^2-(mim^{Ph})-(mim$^{Bu^t}$)]CoCl$_2$ was measured as a function of temperature (Table 6) from which values of ΔH and ΔS were obtained from a van't Hoff plot.

S−S Bond Metathesis between [κ^2-(mim$^{Bu^t}$)$_2$]ZnCl$_2$ and [κ^2-(mim^{Ph})$_2$]ZnCl$_2$. A solution of [κ^2-(mim$^{Bu^t}$)$_2$]ZnCl$_2$ (0.020 g, 0.045 mmol) in CH_2Cl_2 (0.5 mL) was added to a solution of [κ^2-(mim^{Ph})$_2$]-ZnCl$_2$ (0.022 g, 0.045 mmol) in CH_2Cl_2 (0.5 mL). The mixture was transferred to a Teflon-capped NMR tube (J-Young) and monitored by ^{1}H NMR spectroscopy, thereby demonstrating that an equilibrium mixture with [κ^2-(mim^{Ph})(mim$^{Bu^t}$)]ZnCl$_2$ was reached over a period of ca. 1 day at room temperature, although it was not possible to obtain a reliable value for the equilibrium constant because of overlapping of signals for the different species. A mass spectrum obtained from the reaction mixture in CH_2Cl_2 revealed the formation of three molecular ions, *m*/*z* 409.2 {[κ^2-(mim$^{Bu^t}$)$_2$]-ZnCl$_2$ − Cl}$^+$, 429.1 {[κ^2-(mim^{Ph})(mim$^{Bu^t}$)]ZnCl$_2$ − Cl}$^+$, and 451.1 {[κ^2-(mim^{Ph})$_2$]ZnCl$_2$ − Cl}$^+$, consistent with the proposed metathesis.

S−Se Bond Metathesis between [κ^2-(mim$^{Bu^t}$)$_2$]CoCl$_2$ and [κ^2-(seim^{Mes})$_2$]CoCl$_2$. A solution of [κ^2-(mim$^{Bu^t}$)$_2$]CoCl$_2$ (0.014 g, 0.032 mmol) in $CDCl_3$ (0.7 mL) containing Cp_2Fe (0.004 g, 0.022 mmol) as an internal standard was added to a solution of [κ^2-(seim^{Mes})$_2$]-CoCl$_2$ (0.021 g, 0.032 mmol) in $CDCl_3$ (0.7 mL). The mixture was transferrred to a Teflon-capped NMR tube (J-Young) and monitored by ^{1}H NMR spectroscopy, thereby demonstrating that an equilibrium mixture with [κ^2-(mim$^{Bu^t}$)(seim^{Mes})]CoCl$_2$ was reached over a period of ca. 24 h at room temperature. ^{1}H NMR data for [κ^2-(mim$^{Bu^t}$)(seim^{Mes})]CoCl$_2$ ($CDCl_3$): δ 73.6 [s, 2H, Im], 56.8 [s, 1H, Im], 39.5 [s, 1H, Im], 8.30 [s, 2H, *m*-Mes], 2.83 [s, 9H, Bu^t], 2.55 [s, 3H, *p*-CH_3Mes], 1.26 [br s, 6H, *o*-CH_3Mes]. The equilibrium constant for the formation of [κ^2-(mim$^{Bu^t}$)(seim^{Mes})]CoCl$_2$ was measured as a function of temperature (Table 6) from which values of ΔH and ΔS were obtained from a van't Hoff plot.

S−S Bond Metathesis between [κ^2-(mim$^{Bu^t}$)$_2$]CoCl$_2$ and (mim^{Ph})H. A solution of [κ^2-(mim$^{Bu^t}$)$_2$]CoCl$_2$ (0.020 g, 0.045 mmol) in $CDCl_3$ (0.5 mL) was added to a solution of (mim^{Ph})H (0.008 g, 0.045 mmol) in $CDCl_3$ (0.5 mL). The mixture was analyzed by ^{1}H NMR spectroscopy after 20 min, thereby revealing signals indicative of a mixture containing [κ^2-(mim$^{Bu^t}$)$_2$]CoCl$_2$, [κ^2-(mim^{Ph})$_2$]CoCl$_2$, [κ^2-(mim^{Ph})(mim$^{Bu^t}$)]CoCl$_2$, (mim^{Ph})H, and (mim$^{Bu^t}$)H.

X-ray Structure Determinations. X-ray diffraction data were collected on either a Bruker Apex II diffractometer or a Bruker P4 diffractometer equipped with a SMART CCD detector. Crystal data, data collection, and refinement parameters are summarized in Table 7. The structures were solved using direct methods and standard difference map techniques and were refined by full-matrix least-squares procedures on F^2 with *SHELXTL* (versions 5.10 and 6.1).[33]

Computational Details. All calculations were carried out using DFT as implemented in the *Jaguar 6.5* suite of ab initio quantum chemistry programs.[34] Geometry optimizations were performed with the B3LYP density functional[35] and the 6-31G** (C, H, N, P, and S) and LACVP (Ni)[36] basis sets. Cartesian coordinates for geometry-optimized structures are listed in the Supporting Information.

Acknowledgment. We thank the National Institutes of Health (Grant GM046502) for support of this research and for a Postdoctoral Fellowship to J.S.F. (Grant GM074410). Mao Minoura and Victoria K. Landry are thanked for providing a sample of (seim^{Mes})$_2$.

Supporting Information Available: Cartesian coordinates for geometry-optimized structures and crystallographic data in CIF format. This material is available free of charge via the Internet at http://pubs.acs.org.

IC701228Y

(33) Sheldrick, G. M. *SHELXTL, An Integrated System for Solving, Refining and Displaying Crystal Structures from Diffraction Data*; University of Göttingen: Göttingen, Federal Republic of Germany, 1981.
(34) *Jaguar 6.5*, Schrödinger, LLC: New York, 2005.
(35) (a) Becke, A. D. *J. Chem. Phys.* **1993**, *98*, 5648−5652. (b) Becke, A. D. *Phys. Rev. A* **1988**, *38*, 3098−3100. (c) Lee, C. T.; Yang, W. T.; Parr, R. G. *Phys. Rev. B* **1988**, *37*, 785−789. (d) Vosko, S. H.; Wilk, L.; Nusair, M. *Can. J. Phys.* **1980**, *58*, 1200−1211. (e) Slater, J. C. *Quantum Theory of Molecules and Solids, Vol. 4: The Self-Consistent Field for Molecules and Solids*; McGraw-Hill: New York, 1974.
(36) (a) Hay, P. J.; Wadt, W. R. *J. Chem. Phys.* **1985**, *82*, 270−283. (b) Wadt, W. R.; Hay, P. J. *J. Chem. Phys.* **1985**, *82*, 284−298. (c) Hay, P. J.; Wadt, W. R. *J. Chem. Phys.* **1985**, *82*, 299−310.